Achieving Full Diversity in Multi-Antenna Two-Way Relay Networks via Symbol-Based Physical-Layer Network Coding

Ruohan Cao, Tiejun Lv, *Senior Member, IEEE*, Hui Gao, Shaoshi Yang, and John M. Cioffi, *Fellow, IEEE*

***Abstract*—This paper considers physical-layer network coding (PNC) with M-ary phase-shift keying (MPSK) modulation in two-way relay channel (TWRC). A low complexity detection technique, termed symbol-based PNC (SPNC), is proposed for the relay. In particular, attributing to the outer product operation imposed on the superposed MPSK signals at the relay, SPNC obtains the network-coded symbol (NCS) straightforwardly without having to detect individual symbols separately. Unlike the optimal multi-user detector (MUD) which searches over the combinations of all users' modulation constellations, SPNC searches over only one modulation constellation, thus simplifies the NCS detection. Despite the reduced complexity, SPNC achieves full diversity in multi-antenna relay as the optimal MUD does. Specifically, antenna selection based SPNC (AS-SPNC) scheme and signal combining based SPNC (SC-SPNC) scheme are proposed. Our analysis of these two schemes not only confirms their full diversity performance, but also implies when SPNC is applied in multi-antenna relay, TWRC can be viewed as an effective single-input multiple-output (SIMO) system, in which AS-PNC and SC-PNC are equivalent to the general AS scheme and the maximal-ratio combining (MRC) scheme. Moreover, an asymptotic analysis of symbol error rate (SER) is provided for SC-PNC considering the case that the number of relay antennas is sufficiently large.**

***Index Terms*—Physical-layer network coding (PNC), single-input multiple-output (SIMO), two-way relay, multi-antenna relay, diversity analysis.**

I. Introduction

TWO-WAY relay (TWR) is a promising technique to improve the coverage and the connectivity of the half-duplex relay aided networks [1]–[3]. In a three-node network considered as the typical TWR channel (TWRC) [4] [5], the two source nodes exchange information simultaneously with the aid of the relay node. With no direct link between the two source nodes, the communication takes place in the following two phases. In the multiple-access (MA) phase, the source nodes transmit their respective signals to the relay node simultaneously. Then the relay node broadcasts the processed signals to the source nodes in the broadcast (BC) phase. In TWR scenarios, each source node can cancel self-interference, namely the signal sent by itself in the MA phase, from the signal received in the BC phase to recover the information sent by the other source node. This concept is reminiscent of the work on network coding [6]. As a result, the TWR scheme assisted by network coding in analog or digital domain [6] is of particular interest to the research community. On the other hand, wireless channels usually suffer from time-varying fading, resulting in serious performance degradation. According to information theory, a multi-antenna relay can bring diversity gain to the TWR system having two single-antenna end nodes [7]. This paper thus focuses on the diversity technique in network coding aided multi-antenna TWR systems.

In multi-antenna TWR systems, the diversity gain can be achieved by several different methods [8]–[14]. These methods vary in complexity and performance. A low-complexity choice is given by a relay-antenna-selection-aided amplify-and-forward (AF) strategy [9] [10]. Specifically, only one antenna is selected from the multiple antennas of the relay so that the worse received signal-to-noise ratio (SNR) of the two source nodes is maximized. The selected antenna amplifies and forwards its received signal that is corrupted by the noise. This AF-based scheme is shown to provide a diversity gain on the order of the number of relay antennas, namely it achieves full diversity performance [9]. Alternatively, the decode-and-forward (DF) based scheme also achieves full diversity with the aid of maximum likelihood (ML) based multiuser detector (MUD), by which the information bits of the two source nodes are estimated separately, and then conflated to a network-coded symbol (NCS) [11] [12]. Furthermore, compared to the AF based scheme, the DF based scheme can increase the SNR of each source node, because the ML-based MUD actually mitigates the effect of noise in relay node. The increased SNR is obtained at the cost of the complexity of the ML-based MUD, which requires testing as many hypotheses as the square of the modulation order. It is noted that the relay only needs the network-coded information, which inspires us

Manuscript received August 16, 2012; revised February 1, 2013; accepted May 14, 2013. The associate editor coordinating the review of this paper and approving it for publication is D. Tuninetti.

R. Cao and T. Lv are with the School of Information and Communication Engineering (SICE), Beijing University of Posts and Telecommunications (BUPT), Beijing 100876, China (e-mail: {caoruohan, lvtiejun}@bupt.edu.cn).

H. Gao is with Singapore University of Technology and Design, 20 Dover Drive, 138682, Singapore (e-mail: hui_gao@sutd.edu.sg).

S. Yang is with the School of Electronics and Computer Science, University of Southampton, SO17 1BJ Southampton, U.K., and also with the School of Information and Communication Engineering, Beijing University of Posts and Telecommunications (BUPT), Beijing 100876, China (e-mail: sy7g09@ecs.soton.ac.uk).

J. M. Cioffi is with the Department of Electrical Engineering, Stanford University, Stanford, CA, USA (email: cioffi@stanford.edu).

This paper was presented in part at the 2011 IEEE Global Communications Conference (GLOBECOM) and the 2011 IEEE Military Communications Conference (MILCOM). This work is supported by the National Natural Science Foundation of China (NSFC) (Grant No. 61271188), and the China Information Technology Designing Consulting Institute Corporation (CITC) - BUPT SICE Excellent Ph.D. Students Foundation.

Digital Object Identifier 10.1109/TWC.2013.13.121223

to develop a low-complexity denoising technique for direct extraction of the network-coded information without employing the relatively complicated ML-based MUD. This motivation is reminiscent of the notion of physical-layer network coding (PNC) [15].

The PNC is typically dependent on specific modulation constellation, and it is originally proposed for single-antenna TWRC without considering channel fading. In this case, the network coding operation is performed naturally on the superimposed electromagnetic (EM) wave [16]. Due to this fact, PNC-specific detectors are investigated for directly transforming the received EM waves to the network-coded information without detecting bits separately. This idea is then further developed under more general conditions to obtain network-coded information [17]–[21]. The network-coded information herein may refer to two concepts, namely the network-coded bits (NCBs) and the NCSs generated by the network coding operation on bits and on symbols, respectively. Relying on this wisdom, significant efforts have been invested to map the received signal to NCBs firstly and then modulate them as NCSs [15] [18] [19]. By contrast, some other works indicate that NCSs can be straightforwardly obtained by processing the norm of the received signal [20] [21]. However, these schemes all focus on the additive white Gaussian noise (AWGN) channel. When it comes to fading channel, PNC schemes have to employ MUD, which performs explicit detection of the individual symbols sent by the two source nodes [16]. Furthermore, the practical full-diversity oriented PNC-specific detectors are only applicable to binary phase-shift keying (BPSK) modulation [22]. They cannot be generalized to complex-valued modulations. Therefore, there is a great demand for developing the spatial-diversity oriented PNC-specific detectors which are applicable to more general modulation schemes.

In this paper, we conceive a symbol-based PNC (SPNC) technique for M-ary phase-shift keying (MPSK) modulation. SPNC constructs NCSs straightforwardly by processing the outer product of the received signal(s). More specifically, the NCS is defined as the conjugate product of two transmitted symbols, and the proposed network coding operation is performed naturally on the outer product of the received signal(s). The ML-based PNC-specific detectors are developed to extract the NCSs from the outer product. To elaborate a little further, we initially propose a ML-based PNC-specific detector for the single-antenna relay, and then extend it to the multi-antenna relay. Actually the PNC-specific detectors only evaluate all possible NCSs rather than search over all possible combinations of two transmitted symbols as the ML-based MUD usually does. The size of the search space in the ML-based MUD is the square of the modulation order. By contrast, the PNC-specific detectors reduce the search space to one transmitted constellation of one link, whose size is equal to the modulation order[1]. Despite the reduced search space, PNC-specific detectors achieve the same diversity performance as the ML-based MUD. The basic idea of SPNC was partially presented in the conference versions of this paper [23] [24]; however, the ML-based PNC-specific detector was not developed therein, and the analytical diversity performance was not provided either. This paper further extends the contributions of [23] [24] by developing the ML-based PNC-specific detectors and providing the diversity performance analysis. Specifically, the main contributions of this paper are listed as follows.

1) First, we examine the diversity performance of SPNC applied to single-antenna TWRC. In this scenario our analysis shows that the proposed single-antenna PNC-specific detector achieves a diversity order of $\frac{1}{2}$. Moreover, we analyze how the amplitude and the angle of TWRC impact the diversity performance. According to our analysis, the effective angle and the effective amplitude are derived. And we show that the randomness of the effective angle degrades the achievable diversity.

2) Second, we consider SPNC in multi-antenna relay that provides multiple transmission links. Invoking phase alignment (PA) preprocessing, a relay antenna selection aided SPNC scheme is proposed, which is termed AS-SPNC. To be specific, the link with the largest effective amplitude is selected to employ the single-antenna PNC-specific detector, and the randomness of the effective angle of the selected link is removed by PA preprocessing. Both the diversity analysis and simulation results demonstrate that AS-SPNC can achieve full diversity.

3) Third, with the aid of PA preprocessing, an approach for combining the received signals of all links and calculating the outer product of the combined signals is proposed, which is termed signal combining based SPNC (SC-SPNC). The asymptotic analysis demonstrates that SC-SPNC is equivalent to the maximum-ratio-combining (MRC) of NCSs in term of the diversity-achieving capability. Therefore, SC-SPNC is capable of achieving full diversity gain.

Besides the aforementioned novel contributions, we provide a quantitative analysis on the computational complexity. The rest of the paper is organized as follows. In Section II, we describe the traditional MUD based PNC scheme. In Section III, we investigate SPNC in single-antenna TWRC as a preliminary. In Section IV, we focus on SPNC in multi-antenna relay. In Section V, with the aid of the proposed PA strategy, the AS-SPNC and the SC-SPNC are developed and analyzed. In Section VI, numerical results are given to confirm the advantages of the proposed schemes and to validate the theoretical results of diversity order analysis. Finally, Section VII concludes this paper[2].

II. System Model

We first consider a two-way relay network as shown in Fig. 1 where two single-antenna source nodes N_i $(i = 1, 2)$ exchange messages with the aid of the relay node N_3 equipped

[1]For example, with MPSK at each source, MUD requires testing M^2 hypotheses, while PNC-specific detectors only have to evaluate M hypotheses.

[2]In this paper, $(\cdot)^H$,$(\cdot)^T$, $(\cdot)^{-1}$, $\|\cdot\|$ and $\det(\cdot)$ represent the conjugate transpose, transpose, inverse, Frobenius norm, and the determinant of a matrix, respectively. $\Re(\cdot)$, $\Im(\cdot)$, $|\cdot|$ and $(\cdot)^*$ denote the real part, the imaginary part, absolute value and conjugate of a complex-valued variable, respectively. $\mathcal{CN}(\mu, \mathbf{K})$ denotes a complex Gaussian random vector with mean μ and covariance matrix $\mathbf{K}$. $(\cdot)_{2\pi}$ denotes modulo-2π operation. $\angle\cdot$ denotes the angle of a complex-valued number. $\mathbf{A}(\cdot,\cdot)$ represents the entries of $\mathbf{A}$. $\mathbf{0}_{(\cdot)}$ denotes the matrix whose entries are all zero and dimension is shown in subscript. $\mathbf{I}_{(\cdot)}$ denotes the unit matrix and its dimension is shown in subscript. Finally, $\oplus$ denotes bitwise XOR operation.

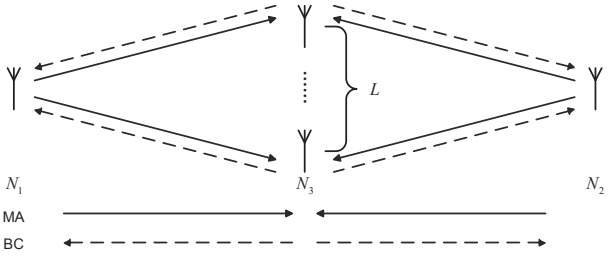

Fig. 1. System model.

with $L \geq 1$ antennas. In this paper we will examine the SPNC technique for the scenarios of $L = 1$ and $L > 1$, respectively. There is no direct link connecting the source nodes. The link between N_i and N_3 is characterized by the $L \times 1$ channel vector $\mathbf{h}_i$, whose elements h_{il} denotes the channel coefficient of the link from source node N_i $(i = 1, 2)$ to the lth $(l = 1, \ldots, L)$ receive antenna of the relay, and h_{il} follows independent identically distributed $\mathcal{CN}(0, 1)$. We assume that the channels are static during the two transmission phases of many consecutive packets, and that the global channel state information (CSI) is perfectly known to the relay node. We consider the following system model throughout this paper. The source node N_i transmits the symbol $x_i \triangleq \sqrt{P}u_i s_i$, where s_i is the modulated symbol and carries the information bits W_i according to the mapping rule $\mathcal{M}$, i.e., $s_i = \mathcal{M}(W_i)$, P is the transmit power, and u_i denotes the preprocessing on s_i. Since MPSK modulation is employed, $s_i \in \Omega$ where $\Omega = \left\{\phi_k = \exp\left(j\frac{2\pi}{M}k\right) : k = 1, \ldots, M\right\}$ is the set of all MPSK constellation symbols and $j = \sqrt{-1}$. It is easy to see that $\phi_k \cdot \phi_k^* = 1$, $\phi_k^* \in \Omega$, and $\phi_{k'} \cdot \phi_k \in \Omega$, where $k, k^{'} = 1, \ldots, M$. The transmission of PNC consists of the MA phase and BC phase. In the MA phase, the superimposed signals are assumed to arrive at the relay node simultaneously. Then the received baseband signal vector is given by

$$\mathbf{y} = \mathbf{h}_1 x_1 + \mathbf{h}_2 x_2 + \mathbf{n}, \tag{1}$$

where $\mathbf{n}$ is the complex Gaussian noise vector at the relay node, and it obeys $\mathcal{CN}\left(\mathbf{0}_{L\times 1}, \sigma^2 \mathbf{I}_{L\times L}\right)$.

In the existing MUD-PNC scheme [11], which is actually a DF-based scheme, the relay node employs the ML-based MUD to jointly decode both messages from $\mathbf{y}$, i.e.,

$$\left(\hat{W}_1, \hat{W}_2\right) = \arg \min_{(W_1,W_2)\in\mathcal{X}\times\mathcal{X}} |\mathbf{y} - \sqrt{P}u_1\mathcal{M}(W_1)\mathbf{h}_1 - \sqrt{P}u_2\mathcal{M}(W_2)\mathbf{h}_2|^2, \tag{2}$$

where $\hat{W}_i$ is the estimate of W_i, $\mathcal{X}$ is the set of all possible bit vectors W_i transmitted by a single antenna, (W_1, W_2) is the element of the Cartesian product of $\mathcal{X}$ and $\mathcal{X}$. The ML-based MUD is employed to achieve full diversity in the MA phase. Based on the result of (2), the NCS is generated by $\mathcal{M}\left(\left[\hat{W}_1 \oplus \hat{W}_2\right]\right)$. Upon broadcasting the NCS via a selected antenna at relay, the end-to-end symbol error rate (SER) performance exhibiting full diversity is achieved in [11]. It is noted that the ML-based MUD in (2) has to search over M^2 elements from $\mathcal{X} \times \mathcal{X}$ to obtain $\left(\hat{W}_1, \hat{W}_2\right)$. In contrast to $(W_1, W_2) \in \mathcal{X} \times \mathcal{X}$ which has M^2 possibilities, the NCS is an element of Ω which has only M possibilities. This observation indicates that the number of NCS candidates is lower than that of (W_1, W_2). However, the complexity cost of determining NCS is the same as that of determining (W_1, W_2) in MUD-PNC. For the sake of low complexity implementation, a specific PNC detection technique shrinking the effective search space of NCS to Ω is proposed in this paper.

III. SPNC in Single-Antenna TWRC

For constructing the NCS, network coding operation should be performed on physical EM waves. The proposed SPNC schemes process outer product of the received signal(s) to generate the NCS directly. As a preliminary, in this section we will examine SPNC in single-antenna TWRC where all nodes are equipped with single antenna. Based on the analysis given in this section, the SPNC will be extended to the multi-antenna relay scenario.

A. Single-Antenna PNC-Specific Detector

When there is no preprocessing at the transmitter, i.e., $u_i = 1$, and $L = 1$, (1) can be rewritten as

$$y = \sqrt{P}h_1 s_1 + \sqrt{P}h_2 s_2 + n, \tag{3}$$

where y, h_i and n are the scalar versions of the received signal, the channel coefficient and the noise defined in Section II, respectively. yy^* is expressed as

$$\begin{aligned} yy^* &= |\sqrt{P}h_1 s_1 + \sqrt{P}h_2 s_2 + n|^2 \\ &= |\left(\sqrt{P}h_1 s_1 s_2^* + \sqrt{P}h_2 + s_2^* n\right) s_2|^2. \end{aligned} \tag{4}$$

Then we define the NCS as

$$s_{NC} = s_1 s_2^*. \tag{5}$$

It is noted that s_2 is an MPSK modulated symbol, i.e., $|s_2|^2 = 1$. Hence, (4) can be written as

$$yy^* = |\sqrt{P}h_1 s_{NC} + \sqrt{P}h_2 + s_2^* n|^2. \tag{6}$$

Because we have

$$\begin{aligned} \Pr(s_{NC} = \phi_k, s_2 = \phi_{k'}) &= \Pr(s_1 = \phi_k\phi_{k'}, s_2 = \phi_{k'}) \\ &= \frac{1}{M^2} = \Pr(s_{NC} = \phi_k)\Pr(s_2 = \phi_{k'}), \end{aligned} \tag{7}$$

s_2 and $\breve{n} \triangleq n s_2^*$ are independent of s_{NC}. Due to the isotropic behavior of the Gaussian random variable n, $\breve{n}$ is Gaussian as well. Then, (6) can be written as

$$yy^* = |\sqrt{P}h_1 s_{NC} + \sqrt{P}h_2 + \breve{n}|^2. \tag{8}$$

The derivation in (8) establishes a straightforward relationship between the NCS s_{NC} and the physical signal yy^*. Because $s_{NC} \in \Omega$, there are M possible candidates for s_{NC}. However, the ML-based MUD represented by (2) has to evaluate M^2 candidates in order to obtain s_{NC}. From this perspective, the size of the search space of the proposed method is reduced from M^2 to M. Note that the search space is simplified by utilizing the constant modules of MPSK signals regardless of the specific values of the channel coefficients of two

links, which allows the proposed scheme to be applicable to the scenario of unbalanced channel states. This is a striking difference between the proposed scheme and the existing schemes which are only applicable when the quality of two links are balanced [18] [19]. According to the ML criterion, the estimate of s_{NC} obtained by using yy^* is given as

$$\hat{s}_{NC} = \arg\max_{\phi_k \in \Omega} \Pr\left(yy^* \mid s_{NC} = \phi_k\right). \tag{9}$$

For each $s_{NC} = \phi_k$, $\sqrt{yy^*} = |\sqrt{P}h_1 s_{NC} + \sqrt{P}h_2 + \breve{n}|$ follows Rice distribution as

$$\Pr\left(\sqrt{yy^*} \mid s_{NC} = \phi_k\right) = \frac{2\sqrt{yy^*}\exp\left(-\frac{yy^*+\mu^2}{\sigma^2}\right)}{\sigma^2} I_0\left(\frac{\sqrt{yy^*}\mu}{\sigma^2}\right), \tag{10}$$

where $\mu = |\sqrt{P}h_1\phi_k + \sqrt{P}h_2|$, $I_0(\cdot)$ is the first kind of zero order modified Bessel function. Substituting (10) into (9), we have

$$\hat{s}_{NC} = \arg\max_{\phi_k \in \Omega} \left(\frac{\exp\left(-\frac{yy^*+\mu^2}{\sigma^2}\right)}{\sigma^2} I_0\left(\frac{\sqrt{yy^*}\mu}{\sigma^2}\right)\right). \tag{11}$$

This is the theoretically optimal detector based on yy^*, where $I_0(\cdot)$ cannot be represented in closed form. For the simplicity of analysis and implementation, we develop the following practical detector based on yy^*. Let us expand (8) as

$$\begin{aligned} yy^* &= c + Ps_1 s_2^* h_2^* h_1 + Ps_2 s_1^* h_2 h_1^* + n^* n \\ &\quad + \sqrt{P}\left(h_1 s_1 + h_2 s_2\right)^* n + \sqrt{P} n^* \left(h_1 s_1 + h_2 s_2\right), \end{aligned} \tag{12}$$

where $c = Ph_1^* h_1 + Ph_2^* h_2$ is a constant. (12) can be rewritten as

$$\begin{aligned} yy^* &= c + Ps_{NC} h_2^* h_1 + Ps_{NC}^* h_2 h_1^* + n^* n + \\ &\sqrt{P}\left(s_1 s_2^* h_1 + h_2\right)^* n s_2^* + \sqrt{P} n^* s_2 \left(s_1 s_2^* h_1 + h_2\right) \\ &= c + 2P\Re\left(\rho s_{NC}\right) + 2\sqrt{P}\Re\left(h^* \breve{n}\right) + n^* n, \end{aligned} \tag{13}$$

where $\rho = h_2^* h_1$ and $h_{s_{NC}} = s_{NC} h_1 + h_2$. Since $n^* n$ is not dominant in (13), $n^* n$ will be neglected in yy^* to facilitate the analysis [25]. Then, yy^* can be approximated as

$$yy^* \simeq c + 2P\Re\left(\rho s_{NC}\right) + 2\sqrt{P}\Re\left(h_{s_{NC}}^* \breve{n}\right). \tag{14}$$

For each $s_{NC} = \phi_k$, yy^* follows the Gaussian distribution of

$$\begin{aligned} &\Pr\left(yy^* \mid s_{NC} = \phi_k\right) \\ &= \frac{1}{\sqrt{4\pi |h_{\phi_k}|^2 \sigma^2 P}} \exp\left(-\frac{\left|yy^* - c - 2P\Re\left(\rho\phi_k\right)\right|^2}{4|h_{\phi_k}|^2 \sigma^2 P}\right), \end{aligned} \tag{15}$$

where $h_{\phi_k} = \phi_k h_1 + h_2$. Finally, the practical detector is expressed as

$$\hat{s}_{NC} = \arg\max_{\phi_k \in \Omega} \frac{1}{\sqrt{|h_{\phi_k}|^2}} \exp\left(-\frac{\left|yy^* - c - 2P\Re\left(\rho\phi_k\right)\right|^2}{4|h_{\phi_k}|^2 \sigma^2 P}\right). \tag{16}$$

As shown in (11) and (16), the proposed PNC-specific detectors extract the NCS based on the norm of the received signal, similar to the existing scheme of [21]. It should be noted that the scheme of [21] requires a threshold value for hard decoding based on the norm. Therefore, it cannot deal with complex-valued signal. In other words, neither can the scheme of [21] be applied in fading single-antenna and multi-antenna TWR systems where the channel coefficients are complex, nor can it be used for the complex-valued MPSK modulation. By contrast, the proposed detector represented by (16) can cope with the complex-valued MPSK modulation signals used in fading channel, and it can be easily extended to multi-antenna scenarios as well. Simulation results in Section V show that the practical detector of (16) and the theoretical detector of (11) achieve a similar error rate performance, which coincides with the diversity order of $\frac{1}{2}$. Our analysis of the diversity performance of (16) is given as follows.

B. Diversity Analysis for Single-Antenna PNC-Specific Detector

In this section, we will give the achievable diversity of the PNC-specific detector of (16). Based on (15), when ϕ_k is the intended symbol, the upper bound of the pairwise error probability (PEP) of confusing ϕ_k with $\phi_{k'}$ conditioned on h_1 and h_2 is expressed as

$$\Pr\left(\phi_k \to \phi_{k'} | h_1, h_2\right) \le \exp\left(-\frac{SNR|\Re\left(h_2^* h_1\left(\phi_k - \phi_{k'}\right)\right)|^2}{4\left(|h_1| + |h_2|\right)^2}\right), \tag{17}$$

where $SNR \triangleq \frac{P}{\sigma^2}$. The proof of (17) can be found in Appendix A. Then, a lemma is given as follows.

Lemma 1: Due to the randomness of the included angle between the bidirectional channels, the lower bound of the achievable diversity order is degraded to $\frac{1}{2}$.

Proof: For the simplicity of analysis, $|\Re\left(h_2^* h_1\left(\phi_k - \phi_{k'}\right)\right)|^2$ is rewritten as

$$|\Re\left(h_2^* h_1\left(\phi_k - \phi_{k'}\right)\right)|^2 = |h_1|^2 |h_2|^2 |d_{kk'}|^2 \cos^2\theta_{kk'}, \tag{18}$$

where $d_{kk'} = \phi_k - \phi_{k'}$, and $\theta_{kk'} = \left(\angle h_1 - \angle h_2 + \angle d_{kk'}\right)_{2\pi}$. $\angle h_1 - \angle h_2$, denoted as θ, is the included angle between the channels, and it is termed as effective angle in this paper. According to [26], both $\angle h_1$ and $\angle h_2$ follow uniform distribution in the domain of $[0, 2\pi]$, and are statistically independent of $|h_1|$ and $|h_2|$. θ and $\theta_{kk'}$ are thus statistically independent of $|h_1|$ and $|h_2|$. Based on the Lemma 1 in [27], θ and $\theta_{kk'}$ also follow uniform distribution over $[0, 2\pi]$.

It is noted that $\frac{|h_1|^2|h_2|^2}{(|h_1|+|h_2|)^2} \ge \frac{\min\left(|h_1|^2, |h_2|^2\right)}{4}$. Substituting (18) into (17), we have

$$\Pr\left(\phi_k \to \phi_{k'} | h_1, h_2\right) \le \exp\left(-\frac{SNR|d_{kk'}|^2 \xi \cos^2\theta_{kk'}}{16}\right), \tag{19}$$

where $\xi = \min\left(|h_1|^2, |h_2|^2\right)$ follows exponential distribution, and is statistically independent of $\theta_{kk'}$. ξ is defined as the effective amplitude of the single-antenna TWRC. By making the averaging operation with respect to $\theta_{kk'}$ and ξ, we get

$$\begin{aligned} \Pr\left(\phi_k \to \phi_{k'}\right) &\le \mathbb{E}_{\theta,\xi}\left\{\exp\left(-\frac{SNR|d_{kk'}|^2 \xi \cos^2\theta}{16}\right)\right\} \\ &= \mathbb{E}_\theta \mathbb{E}_\xi \left\{\exp\left(-\frac{SNR|d_{kk'}|^2 \xi \cos^2\theta}{16}\right)\right\}, \end{aligned} \tag{20}$$

where the equality holds because 1) ξ and $\theta_{kk'}$ are statistically independent of each other; 2) $\theta_{kk'}$ and θ follow identical distribution, hence they are mutually replaceable in the expectation

operation. As shown in (20), its right-hand side can be easily calculated by averaging with respect to ξ and θ in turn, which provides insight to the impact imposed by ξ and θ on the diversity performance. To be more specific, we have

$$\mathbb{E}_{\xi}\left\{\exp\left(-\frac{SNR|d_{kk'}|^2\xi\cos^2\theta}{16}\right)\right\}=\frac{32}{32+SNR|d_{kk'}|^2\cos^2\theta}, \tag{21}$$

and then,

$$\begin{aligned}\mathbb{E}_{\theta}\left\{\frac{32}{32+SNR|d_{kk'}|^2\cos^2\theta}\right\}&=\frac{1}{2\pi}\int_0^{2\pi}\frac{32}{32+SNR|d_{kk'}|^2\cos^2\theta}d\theta\\&=\frac{\sqrt{32}}{\sqrt{32+SNR|d_{kk'}|^2}}.\end{aligned} \tag{22}$$

Therefore, when SNR is sufficiently high, (20) can be rewritten as

$$\Pr\left(\phi_k\rightarrow\phi_{k'}\right)\leq\frac{\sqrt{32}}{SNR^{\frac{1}{2}}|d_{kk'}|}. \tag{23}$$

■

As shown in (23), the lower bound of the achievable diversity order is $\frac{1}{2}$, which is tight according to our simulation results provided in Section V. The above analysis reveals that the effective amplitude and the effective angle of the TWRC play different roles in achieving diversity. To be more specific, when we only average with respect to ξ, the intermediate result of PEP decreases at a rate of SNR^{-1} as shown in (21). Then, when we average with respect to θ in turn, the ultimate PEP is deteriorated at a rate of $SNR^{-\frac{1}{2}}$ as shown in (22). Comparing the results of (21) and (22), we conclude that the randomness of θ degrades the diversity performance. Besides, referring to (14), we note that in single-antenna TWRC the detector of (16) only takes the real component of ρs_{NC} to construct the decision statistics, which introduces θ that deteriorates the achievable diversity. The above analysis inspires us to cope with the randomness of the effective angle to achieve full diversity in the multi-antenna relay scenario.

IV. SPNC IN MULTI-ANTENNA TWRC

In this section, we investigate multi-antenna TWRC consisting of two single-antenna source nodes and a multi-antenna relay, i.e., $L>1$. We consider the end-to-end diversity gain, i.e., $d\triangleq\lim\limits_{SNR\rightarrow\infty}-\frac{\log P_E}{\log SNR}$, where P_E denotes the overall SER, and it is jointly decided by P_{MA} and P_{BC} which denote the SER performance of MA and BC phases, respectively. Specifically, only if P_{MA} and P_{BC} both exhibit full diversity order, P_E would exhibit full diversity order [28]. The diversity order of both P_{MA} and P_{BC} thus needs to be investigated for obtaining P_E. In this paper, we employ a max-min criterion based antenna selection scheme [12] for BC phase, where P_{BC} has been given in [12] and demonstrated to exhibit full diversity order. As a result, we only need to focus on the SER of the MA phase, which is elaborated on as follows.

For achieving full diversity, two schemes are proposed for multi-antenna TWRC, and both of them are based on the phase alignment (PA) preprocessing. One scheme constructs the NCS from the outer product of the signal received at the selected antenna, and we term it AS-SPNC. The other scheme called SC-SPNC combines the received signals of all antennas to calculate the outer product. The diversity analyses of them are also investigated, which demonstrate that by using the SPNC technique in multi-antenna TWRC, the NCS can be detected as if it were transmitted in an effective single-input multiple-output (SIMO) system.

A. PA Aided Antenna Selection Based SPNC (AS-SPNC)

We first select one antenna of the relay node to perform NCS transmission in the MA phase according to the following criterion

$$\hat{l}=\arg\max_{l=1,\ldots,L}\xi_l, \tag{24}$$

where $\xi_l=\min\left\{|h_{1l}|^2,|h_{2l}|^2\right\}$ is defined as the effective amplitude of the lth transmission link provided by the lth antenna of the relay. (24) is referred to as maximin criterion which is also used in the BC phase [11], [29]. In the MA phase, SPNC achieves full diversity aided by the PA preprocessing, as detailed below.

In general, PA preprocessing is proposed to adjust the included angle between the employed channels to a constant. As a beneficial result, the randomness of the included angle can be removed. Specifically, for the lth antenna is selected, a PA preprocessing strategy is given by

$$u_1=\exp\left(-j\angle h_{1\hat{l}}\right)\exp\left(j\upsilon\right),u_2=\exp\left(-j\angle h_{2\hat{l}}\right), \tag{25}$$

where υ is a constant rotation angle that will be given later. From (25), we see that PA consists of the following two steps: (i) each source node pre-cancels the angle of the channel from itself to the selected relay antenna; (ii) source node N_1 rotates the transmitted constellation symbol by a constant angle υ upon finishing the step (i)[3]. The effect of the two steps will be detailed in the following analysis.

Note that $h_{i\hat{l}}=|h_{i\hat{l}}|\exp\left(j\angle h_{i\hat{l}}\right)$, then the received signal in the $\hat{l}$th relay antenna may be expressed as

$$\begin{aligned}y_{\hat{l}}&=\sqrt{P}h_{1\hat{l}}u_1s_1+\sqrt{P}h_{2\hat{l}}u_2s_2+n_{\hat{l}}\\&=\sqrt{P}|h_{1\hat{l}}|\exp\left(j\upsilon\right)s_1+\sqrt{P}|h_{2\hat{l}}|s_2+n_{\hat{l}},\end{aligned}$$

where $y_{\hat{l}}$ and $n_{\hat{l}}$ denote the received signal and the noise at the $\hat{l}$th relay-antenna, respectively. Applying the single-antenna PNC-specific detector of (16) to $y_{\hat{l}}y_{\hat{l}}^*$, the detection may be viewed as the detection in an equivalent single-antenna TWRC system as aforementioned, where h_1 and h_2 would be substituted by $|h_{1\hat{l}}|\exp\left(j\upsilon\right)$ and $|h_{2\hat{l}}|$, respectively. Following the analysis of (19), the PEP of (16) applied to $y_{\hat{l}}y_{\hat{l}}^*$ is given as

$$\Pr\left(\phi_k\rightarrow\phi_{k'}|h_{1\hat{l}},h_{2\hat{l}}\right)\leq\exp\left(-\frac{SNR\xi_{\hat{l}}|d_{kk'}|^2\cos^2\theta'_{kk'}}{16}\right), \tag{26}$$

where we have $\xi_{\hat{l}}=\min\left(|h_{1\hat{l}}|^2,|h_{2\hat{l}}|^2\right)$, $\theta'_{kk'}=\left(\theta+\angle d_{kk'}\right)_{2\pi}$, and $\theta=\angle|h_{1\hat{l}}|\exp\left(j\upsilon\right)-\angle|h_{2\hat{l}}|$ representing the included angle between $|h_{1\hat{l}}|\exp\left(j\upsilon\right)$ and $|h_{2\hat{l}}|$. Note that $|h_{1\hat{l}}|$ and $|h_{2\hat{l}}|$ are real-valued variables, i.e., $\angle|h_{i\hat{l}}|=0,i=1,2$, hence we have $\theta=\upsilon$ and $\theta'_{kk'}=\left(\upsilon+\angle d_{kk'}\right)_{2\pi}$. We can see that the step (i) in PA preprocessing makes $\theta'_{kk'}$ become a constant

[3]In the practical implement of PA strategy, the relay firstly transmits u_1 and u_2 to N_1 and N_2, respectively. It is noted that u_1 and u_2 carry information about phases whose values always belong to $[0,\ 2\pi]$. As a result, the quantification of u_1 and u_2 won't bring much complexity to the system.

in spite of channel fading for eliminating randomness of θ. After the step (ii), $\theta'_{kk'}$ is associated with the constant rotation angle υ which is given off-line and can be easily designed to make the upper bound of (26) hold. There are many choices[4] of υ capable of avoiding the undesirable condition $\cos^2\theta'_{kk'}=0$. These choices affect power gain rather than diversity gain, because the term $\cos^2\theta'_{kk'}$ decided by υ is a constant coefficient of SNR in (26). On the other hand, in (26), only the effective amplitude of channel $\xi_{\hat{l}}$ is random, and $\xi_{\hat{l}}$ can also be written as

$$\xi_{\hat{l}}=\max\xi_l, l=1,\ldots,L. \tag{27}$$

According to (27), $SNR\cdot\xi_{\hat{l}}$ in (26) can be regarded as the SNR achieved at the selected receive antenna of a virtual SIMO system whose channel amplitudes are $\xi_1,...,\xi_L$. From this perspective, AS-SPNC is equivalent to the NCS detection by means of selecting one receive antenna in the effective SIMO system. Similar to the role of AS in general SIMO system, AS-SPNC can also achieve full diversity in the MA phase according to the following lemma.

Lemma 2: Aided by PA strategy, P_{MA} exhibits the full diversity order when using AS-SPNC.

Proof: See Appendix B. ∎

Then, the maximin criterion (24) is employed again to select a bidirectional broadcast channel, and achieves full diversity performance in the BC phase, the same as what can be achieved in the MA phase. According to [28], the PA aided AS-SPNC scheme is capable of achieving an overall end-to-end full diversity performance. Furthermore, it has been shown that the maximin strategy can achieve full diversity in terms of the outage capacity [29]. However, this theoretically potential diversity cannot be realized with respect to the SER performance by employing the maximin strategy straightforwardly. Actually, if the preprocessing technique is not invoked, the maximin strategy achieves only a diversity order of one with respect to the SER when the complex-valued modulation is used. As shown in our analysis, the PA preprocessing aids the maximin strategy to approach its theoretical potential. Additionally, note that when the channels are reciprocal in MA and BC phases, a common antenna will be selected throughout MA and BC phases, which allows the PA aided AS-SPNC to be extended straightforwardly into a distributed scenario as considered in [30].

B. PA aided signal combination based SPNC (SC-SPNC)

In contrast to the AS based scheme which generates the NCS by using only one selected antenna, in this subsection, we proceed to investigate the scheme fully utilizing all the antennas of the relay.

1) Multi-Antenna PNC-Specific Detector: To simplify implementation, we try to transform the received signal vector $\mathbf{y}$ of dimension $L\times1$ to a vector of constant dimension regardless of the value of L. Because the transformation should keep the energy of $\mathbf{y}$, QR decomposition is employed. To elaborate a little further, the received signal vector (1) is first rewritten as

$$\mathbf{y}=\sqrt{P}\mathbf{h}_1u_1s_1+\sqrt{P}\mathbf{h}_2u_2s_2+\mathbf{n}=\tilde{\mathbf{H}}\tilde{\mathbf{S}}+\mathbf{n},$$

where $\tilde{\mathbf{H}}=[\mathbf{h}_1u_1,\mathbf{h}_2u_2]$ and $\tilde{\mathbf{S}}=\left[\sqrt{P}s_1,\sqrt{P}s_2\right]^T$. Then, we apply the combining matrix $\mathbf{Q}$ at the relay, where $\mathbf{Q}$ is given by the QR decomposition of $\tilde{\mathbf{H}}$, i.e.,

$$\widetilde{\mathbf{H}}=\mathbf{Q}\tilde{\mathbf{R}}=[\mathbf{Q}_1,\mathbf{Q}_2]\left[\begin{array}{c}\mathbf{R}\\ \mathbf{0}_{(L-2)\times2}\end{array}\right]$$

where $\mathbf{Q}_1$ is an $L\times2$ matrix, $\mathbf{Q}_2$ is an $L\times(L-2)$ matrix, $\mathbf{Q}_1^H\mathbf{Q}_1$ and $\mathbf{Q}_2^H\mathbf{Q}_2$ are identity matrices, and $\mathbf{R}$ is a 2×2 upper triangular matrix given as

$$\mathbf{R}=\left[\begin{array}{cc}r_{11}&r_{12}\\0&r_{22}\end{array}\right]\triangleq[\mathbf{r}_1,\mathbf{r}_2], \tag{28}$$

where r_{11} and r_{22} are real numbers, r_{12} is a complex number. Applying $\mathbf{Q}$ to $\mathbf{y}$, we obtain

$$\mathbf{Q}^H\mathbf{y}=\left[\begin{array}{c}\mathbf{R}\\ \mathbf{0}_{(L-2)\times2}\end{array}\right]\left[\begin{array}{c}\sqrt{P}s_1\\ \sqrt{P}s_2\end{array}\right]+\left[\begin{array}{c}\mathbf{Q}_1^H\mathbf{n}\\ \mathbf{Q}_2^H\mathbf{n}\end{array}\right].$$

Furthermore, we have

$$\widetilde{\mathbf{y}}\triangleq\mathbf{Q}_1^H\mathbf{y}=\sqrt{P}\mathbf{r}_1s_1+\sqrt{P}\mathbf{r}_2s_2+\widetilde{\mathbf{n}},$$

where $\widetilde{\mathbf{n}}=\mathbf{Q}_1^H\mathbf{n}$ is also a Gaussian vector variable because $\mathbf{Q}_1^H\mathbf{Q}_1$ is an identity matrix. At the relay node, the outer product $\widetilde{\mathbf{y}}\widetilde{\mathbf{y}}^H$ is calculated as

$$\widetilde{\mathbf{y}}\widetilde{\mathbf{y}}^H=\mathbf{C}+\underbrace{\mathbf{S}_0+\mathbf{N}}_{\mathbf{T}_0}, \tag{29}$$

where $\mathbf{C}=P\left(\mathbf{r}_1\mathbf{r}_1^H+\mathbf{r}_2\mathbf{r}_2^H\right)$ is a constant matrix, $\mathbf{S}_0=P\left(s_{NC}\mathbf{r}_1\mathbf{r}_2^H+s_{NC}^*\mathbf{r}_2\mathbf{r}_1^H\right)$, and

$$\mathbf{N}=\sqrt{P}\left(\mathbf{r}_1s_{NC}+\mathbf{r}_2\right)s_2\widetilde{\mathbf{n}}^H+\sqrt{P}s_2^*\widetilde{\mathbf{n}}\left(\mathbf{r}_1s_{NC}+\mathbf{r}_2\right)^H+\widetilde{\mathbf{n}}\widetilde{\mathbf{n}}^H. \tag{30}$$

Due to the same reason for neglecting n^*n in (13), we can neglect $\widetilde{\mathbf{n}}\widetilde{\mathbf{n}}^H$ in $\mathbf{N}$. As a result, $\mathbf{N}$ may be approximated as

$$\mathbf{N}\simeq\sqrt{P}\mathbf{r}\check{\mathbf{n}}^H+\sqrt{P}\check{\mathbf{n}}\mathbf{r}^H,$$

where $\mathbf{r}=\mathbf{r}_1s_{NC}+\mathbf{r}_2$, $\check{\mathbf{n}}=s_2^*\widetilde{\mathbf{n}}$. Due to the isotropic behavior of $\widetilde{\mathbf{n}}$, $\check{\mathbf{n}}=s_2^*\widetilde{\mathbf{n}}$ is Gaussian as well, because the elements of $\widetilde{\mathbf{n}}$ are independent identically distributed $\mathcal{CN}\left(0,\sigma^2\right)$. According to (7), s_2 is statistically independent of s_{NC}, hence $\widetilde{\mathbf{n}}$ is independent of $\mathbf{r}$. Based on the stochastic property of $\mathbf{N}$ presented hereinbefore, the ML detector for $\widetilde{\mathbf{y}}\widetilde{\mathbf{y}}^H$ can be obtained.

Substituting (28) into (29), we have

$$\mathbf{T}_0=P\left[\begin{array}{cc}2\Re\left(r_{11}r_{12}^*s_{NC}\right)&r_{11}r_{22}s_{NC}\\ r_{11}r_{22}s_{NC}^*&0\end{array}\right]+\mathbf{N}.$$

It is straightforward to see that $\mathbf{S}_0(2,2)=0$, which indicates that $\mathbf{T}_0(2,2)$ does not contain any information of s_{NC}. Additionally, we have $\mathbf{T}_0(1,2)=\mathbf{T}_0^*(2,1)$, which implies that $\mathbf{T}_0(2,1)$ and $\mathbf{T}_0(1,2)$ have the same information of s_{NC}. For detecting s_{NC}, $\mathbf{T}_0$ is transformed into a vector of $\mathbf{t}$, i.e.,

$$\mathbf{t}=\left(\mathbf{T}_0(1,1),\Re\left(\mathbf{T}_0(1,2)\right),\Im\left(\mathbf{T}_0(1,2)\right)\right)^T=\mathbf{s}_e+\mathbf{n}_e,$$

where $\mathbf{s}_e=\left(\mathbf{S}_0(1,1),\Re\left(\mathbf{S}_0(1,2)\right),\Im\left(\mathbf{S}_0(1,2)\right)\right)^T$ and $\mathbf{n}_e=\left(\mathbf{N}(1,1),\Re\left(\mathbf{N}(1,2)\right),\Im\left(\mathbf{N}(1,2)\right)\right)^T$. Then, the ML-based detection of s_{NC} is given by

$$\hat{s}_{NC}=\arg\max_{\phi_k\in\Omega}\Pr\left(\mathbf{n}_e=\mathbf{t}-\mathbf{s}_e\left(s_{NC}\right)\mid s_{NC}=\phi_k\right). \tag{31}$$

From (29), $\mathbf{s}_e$ is a constant matrix when there is $s_{NC}=\phi_k$, hence it is denoted as $\mathbf{s}_e\left(s_{NC}\right)$. Each entry of $\mathbf{n}_e$

[4]The optimal υ can be calculated off-line according to $\arg\max_{\upsilon'\in[0,2\pi]}\min_{\phi_k,\phi_{k'}\in\Omega}\cos^2(\upsilon'+\angle(\phi_k-\phi_{k'}))_{2\pi}$.

can be expressed as the linear summation of $\bar{\mathbf{n}} = (\Re(\check{\mathbf{n}}(1)), \Im(\check{\mathbf{n}}(1)), \Re(\check{\mathbf{n}}(2)), \Im(\check{\mathbf{n}}(2)))^T$, i.e., $\mathbf{n}_e = \sqrt{P}\mathbf{m}\bar{\mathbf{n}}$, where

$$\mathbf{m} = \begin{bmatrix} 2\Re(\mathbf{r}(1)) & 2\Im(\mathbf{r}(1)) & 0 & 0 \\ \Re(\mathbf{r}(2)) & \Im(\mathbf{r}(2)) & \Re(\mathbf{r}(1)) & \Im(\mathbf{r}(1)) \\ -\Im(\mathbf{r}(2)) & \Re(\mathbf{r}(2)) & \Im(\mathbf{r}(1)) & -\Re(\mathbf{r}(1)) \end{bmatrix}. \tag{32}$$

Therefore, $\mathbf{n}_e$ is a Gaussian random vector whose mean is $\mathbf{0}_{3\times 1}$, and covariance matrix is $\frac{P\sigma^2}{2}\mathbf{m}\mathbf{m}^H$. The PDF of $\mathbf{n}_e$ is thus given by

$$\Pr(\mathbf{n}_e = \mathbf{t} - \mathbf{s}_e(\phi_k) \mid s_{NC} = \phi_k) = \frac{1}{\sqrt{(2\pi)^3 \frac{P\sigma^2}{2} \det(\mathbf{m}\mathbf{m}^H)}} \cdot \cdot \exp\left(-\frac{(\mathbf{t} - \mathbf{s}_e(\phi_k))^T (\mathbf{m}\mathbf{m}^H)^{-1} (\mathbf{t} - \mathbf{s}_e(\phi_k))}{P\sigma^2}\right). \tag{33}$$

Substituting (33) into (31), we obtain the multi-antenna PNC-specific detector given by

$$\hat{s}_{NC} = \arg\max_{\phi_k \in \Omega} \frac{1}{\sqrt{\det(\mathbf{m}\mathbf{m}^H)}} \exp\left(-\frac{(\mathbf{t} - \mathbf{s}_e(\phi_k))^T (\mathbf{m}\mathbf{m}^H)^{-1} (\mathbf{t} - \mathbf{s}_e(\phi_k))}{P\sigma^2}\right). \tag{34}$$

Similar to (16), the multi-antenna PNC-specific detector reduces the effective search space to Ω. When the number of relay antennas is sufficiently large, it also achieves full diversity as proved below.

2) Asymptotic Performance Analysis: It is difficult to derive an exact closed form expression of SER for the detector of (34). As an alternative, we investigate the asymptotic SER of (34) upon considering the scenario where the number of relay antennas becomes large, which can provide some interesting insights. Revisiting (28), based on the property of QR decomposition, we obtain

$$r_{11} = ||\mathbf{h}_1||, r_{12} = \frac{u_1^* u_2 \mathbf{h}_1^H \mathbf{h}_2}{||\mathbf{h}_1||}, \quad and \quad r_{22} = ||u_2\mathbf{h}_2 - r_{12}\frac{u_1\mathbf{h}_1}{||\mathbf{h}_1||}||.$$

Then, we expand $\mathbf{T}_0(1,1)$ and $\mathbf{T}_0(1,2)$ which are utilized to estimate s_{NC} in (34) as

$$\mathbf{T}_0(1,1) = 2P\Re(r_{11}r_{12}^* s_{NC}) + 2\sqrt{P}\Re((r_{11}s_{NC} + r_{12})\check{\mathbf{n}}^*(1)), \tag{35}$$

and

$$\mathbf{T}_0(1,2) = Pr_{11}r_{22}s_{NC} + \sqrt{P}(r_{11}s_{NC} + r_{12})\check{\mathbf{n}}^*(2) + \sqrt{P}r_{22}\check{\mathbf{n}}^*(1), \tag{36}$$

respectively. Comparing (35) and (36), we can make the following remarks.

Remarker 1: The form of (35) is similar to that of (14), in which the NCS s_{NC}, multiplying a complex coefficient, is included in $\Re(\cdot)$. As demonstrated by the analysis in Section III, the operation $\Re(\cdot)$ therein introduces the randomness of the effective angle of the channel, and as a result, the achievable diversity performance would be degraded without PA strategy being used. By contrast, in (36) the NCS s_{NC} appears in $r_{11}r_{22}s_{NC}$ without invoking $\Re(\cdot)$. Therefore, the randomness of the effective angle of the channel can be avoided by processing $\mathbf{T}_0(1,2)$.

Remarker 2: When the number of relay antennas is large, $\mathbf{h}_1^H\mathbf{h}_2$ approximates to zero according to the law of large numbers [31]. Therefore, $r_{12} = \frac{u_1^* u_2 \mathbf{h}_1^H \mathbf{h}_2}{||\mathbf{h}_1||}$ and $r_{11}r_{12}^* = u_2^* u_1 \mathbf{h}_2^H \mathbf{h}_1$ approach zero, and r_{22} approaches $||\mathbf{h}_2||$. As a result, $\mathbf{T}_0(1,1)$ scarcely contains any information of s_{NC} which is multiplied by $r_{11}r_{12}^*$. In such case that L is sufficiently large to neglect $\mathbf{T}_0(1,1)$, $\mathbf{T}_0(1,2)$ thus contains almost all the information about s_{NC}. As a beneficial result, we can investigate the performance of the multi-antenna PNC-specific detector of (34) by only examining the detection of s_{NC} based on $\mathbf{T}_0(1,2)$.

Upon extracting s_{NC} from $\mathbf{T}_0(1,2)$, $\Pr(\mathbf{T}_0(1,2) \mid s_{NC} = \phi_k)$ is given by

$$\Pr(\mathbf{T}_0(1,2) \mid s_{NC} = \phi_k) = \frac{1}{\sqrt{2\pi\left((r_{11}s_{NC} + r_{12})^2 + r_{22}^2\right)\sigma^2}} \cdot \cdot \exp\left(-\frac{|\mathbf{T}_0(1,2) - Pr_{11}r_{22}s_{NC}|^2}{2\left((r_{11}s_{NC} + r_{12})^2 + r_{22}^2\right)\sigma^2 P}\right). \tag{37}$$

Then, the detection of s_{NC} based on $\mathbf{T}_0(1,2)$ is given as

$$\hat{s}_{NC} = \arg\max_{\phi_k \in \Omega} \frac{1}{\sqrt{2\pi\left((r_{11}\phi_k + r_{12})^2 + r_{22}^2\right)\sigma^2}} \cdot \cdot \exp\left(-\frac{|\mathbf{T}_0(1,2) - Pr_{11}r_{22}\phi_k|^2}{2\left((r_{11}\phi_k + r_{12})^2 + r_{22}^2\right)\sigma^2 P}\right). \tag{38}$$

When L becomes large, r_{12} is trivial, and hence the detector (38) may be viewed as the estimate of $Pr_{11}r_{22}s_{NC}$ in the presence of the Gaussian noise with power $\left({r_{11}}^2 + r_{22}^2\right)\sigma^2$. Then, the pairwise SER of (38) is given by

$$\Pr(\phi_k \to \phi_{k'} | \mathbf{h}_1, \mathbf{h}_2) \simeq Q\left(\sqrt{\frac{SNR|d_{kk'}|^2 z}{4}}\right), \tag{39}$$

where $z = \min\left(r_{11}^2, r_{22}^2\right)$. According to the law of large numbers, $z \simeq \frac{2|r_{11}r_{22}|^2}{\left(r_{11}^2 + r_{22}^2\right)}$ when L goes to infinity. By averaging (39) over z, the SER is formulated as

$$P_{MA} = \frac{1}{2M}\sum_{k=1}^{M}\sum_{k'=1,\neq k}^{M}\sum_{p=0}^{L-1}\frac{(L-1+p)!}{(L-1)!p!2^{L-1+p}} \cdot \cdot \left(1 - \sum_{q=0}^{L-1+p}\binom{2q}{q}\varpi\left(\frac{1-\varpi}{2}\right)^q\left(\frac{1+\varpi}{2}\right)^q\right). \tag{40}$$

where $\varpi = \sqrt{\frac{8}{16 + SNR|d_{kk'}|^2}}$. The proof of (40) is given in Appendix C. It should be noted that when L is large enough, since only $\mathbf{T}_0(1,2)$ contains the information about s_{NC}, the detector (38) is asymptotically equivalent to (34). Based on this observation, the performance of (40) may indicate the performance of (34). As will be shown in Section V, our simulation results demonstrate that (40) is rather accurate when the number of relay antennas is more than 4.

To give more insights into the property of the multi-antenna PNC-specific detector when L is large, the diversity performance of (38) is derived below. It is noted that

$$z = \min\left(r_{11}^2, r_{22}^2\right) = \min\left(\sum_{l=1}^{L}|h_{1l}|^2, \sum_{l=1}^{L}|h_{2l}|^2\right) \geq \sum_{l=1}^{L}\min\left(|h_{1l}|^2, |h_{2l}|^2\right) = \sum_{l=1}^{L}\xi_l. \tag{41}$$

Recalling that $\xi_l = \min\left\{|h_{1l}|^2, |h_{2l}|^2\right\}$, and substituting (41) to (39), we have

$$\Pr\left(\phi_k \to \phi_{k'}|\mathbf{h}_1, \mathbf{h}_2\right) \leq Q\left(\sqrt{\frac{SNR|d_{kk'}|^2\sum_{l=1}^{L}\xi_l}{4}}\right)$$
$$\leq \exp\left(-\frac{|d_{kk'}|^2 SNR\sum_{l=1}^{L}\xi_l}{8}\right) = \prod_{l=0}^{L}\exp\left(-\frac{|d_{kk'}|^2 SNR\xi_l}{8}\right). \quad (42)$$

In (42), $SNR\sum_{l=1}^{L}\xi_l$ can be viewed as the SNR achieved by the MRC technique in a virtual SIMO system where s_{NC} is transmitted by one antenna and received by L antennas, and each channel is characterized by ξ_l. Therefore, SC-SPNC is similar to the MRC that combines the information of NCS from all receive antennas in the effective SIMO system. Similar to the MRC schemes in general SIMO system, SC-SPNC can achieve full diversity in the MA phase. Averaging (42) with respect to ξ_l, we have

$$\Pr\left(\phi_k \to \phi_{k'}\right) \leq \prod_{l=0}^{L}\mathbb{E}_{\xi_l}\left\{\exp\left(-\frac{SNR|d_{kk'}|^2\xi_l}{8}\right)\right\} \quad (43)$$
$$= \left(\frac{16}{16 + SNR|d_{kk'}|^2}\right)^L.$$

As SNR increases, (43) becomes as

$$\Pr\left(\phi_k \to \phi_{k'}\right) \leq \frac{1}{SNR^L}\left(\frac{16}{|d_{kk'}|^2}\right)^L, \quad (44)$$

which implies that the diversity order achieved by (38) is at least L. Since the achievable diversity order cannot be more than L [26], (38) thus achieves full diversity order, i.e., L, in the MA phase. The relay then broadcasts $\hat{s}_{NC}$ by employing a maximin-based selection strategy in the BC phase [11], where the BC-phase SER P_{BC} has been given as [12]

$$P_{BC} = \frac{1}{2\pi}\int_0^{\pi-\pi/M}\frac{L!}{\prod_{k=0}^{L-1}\left(k+1+\frac{SNR\sin^2\pi/M}{2\sin^2\theta}\right)}d\theta. \quad (45)$$

According to [12], the overall SER P_E is given by

$$P_E = P_{MA} + P_{BC}, \quad (46)$$

where P_{MA} represents the SER of the MA phase. Substituting (45) and (40) into (46), P_E can be obtained. Note that P_{MA} and P_{BC} both exhibit full diversity order, P_E thus exhibits full diversity order [28].

3) Complexity Analysis for Multi-Antenna PNC-Specific Detector: As shown in (34), the multi-antenna PNC-specific detector introduces some extra operations. At first glance, it seems that the complexity advantage is not so obvious. To highlight the complexity advantage of the proposed multi-antenna PNC-specific detector, we provide the following quantitative complexity analysis.

In this paper, the complexity is measured by the average number of floating-point operations (FLOPs)[5] cost for each NCS. The total complexity consists of off-line complexity (C_{off}) and on-line complexity (C_{on}). The channel is assumed to be flat fading, which allows the system to calculate some terms at the beginning of each coherence time period. Then, the result is saved and utilized to process each signal until the channel changes. The number of FLOPs cost for the calculation at the beginning of each coherence time period is termed as off-line complexity. The number of FLOPs cost in each instant is termed as on-line complexity. Then, the total complexity can be expressed as $\frac{C_{off}}{N} + C_{on}$, where N is the number of symbols transmitted during a coherence time period, and we have $N \geqslant 10^3$ in practical flat fading system. For comparing the complexity between MUD and the proposed multi-antenna PNC-specific detector, a lemma is given as follows.

[5]Each addition, subtraction, multiplication and division of real-valued numbers cost one FLOP, respectively. Each multiplication operation of complex-valued numbers costs six FLOPs.

TABLE I
COMPLEXITY COMPARISON BETWEEN MUD AND PNC-SPECIFIC DETECTOR

	$L=4$		$L=6$		$L=8$	
	MUD	PNC	MUD	PNC	MUD	PNC
C_{off}	3584	509	5376	571	7168	633
C_{on}	1280	240	1920	272	2560	304
Total	1283.6	240.5	1925.4	272.6	2567.2	304.6
$\frac{C_{pnc}}{C_{mud}}$	18.7%		14.2%		12%	

Lemma 3: $C_{mud} = \frac{14M^2L}{N} + 5M^2L, C_{pnc} = \frac{47M+31L+9}{N} + 21M + 16L + 8$, where C_{mud} and C_{pnc} denote the complexity of MUD and the proposed multi-antenna PNC-specific detector, respectively.

Proof: See Appendix D. ■

Based on the above analytical result, we can give the complexity comparison between MUD and the proposed multi-antenna PNC-specific detector for the setup of "M=8 and N=1000" in Table I. From Table I, we can find that in terms of complexity, the multi-antenna PNC-specific detector has an advantage over MUD. Moreover, this advantage becomes increasingly evident as L increases in a medium range of value, such as from 4 to 8. However, it is noted that when the number of relay antennas becomes (infinitely) large, the two links are orthogonal, and hence the size of search space for MUD is $2M$ rather than M^2. In such case, although the PNC-specific detector does not enjoy significant advantage over MUD in terms of detection efficiency, the PNC technique is still worth being integrated into large-scale system owing to its better capacity efficiency, which, however, is beyond the scope of this paper.

V. SIMULATIONS AND DISCUSSIONS

In this section, we provide simulations to evaluate the performance of the proposed schemes, which also validate our theoretical analysis of the end-to-end diversity order and SER performance. The system model for simulations is shown in Fig. 1, where the relay node is equipped with L antennas. The variance of the complex-valued channel coefficient and of the noise is set to 1.

Fig. 2 focuses on the end-to-end SER performance of the proposed AS-SPNC scheme with different number of relay antennas when we have $M = 4$. To validate the diversity analysis, we measure the diversity order of the simulated curves by using $\beta SNR^{-\alpha}$ as the reference, where β is a case-dependent coefficient and α is a positive number. When SNR is high,

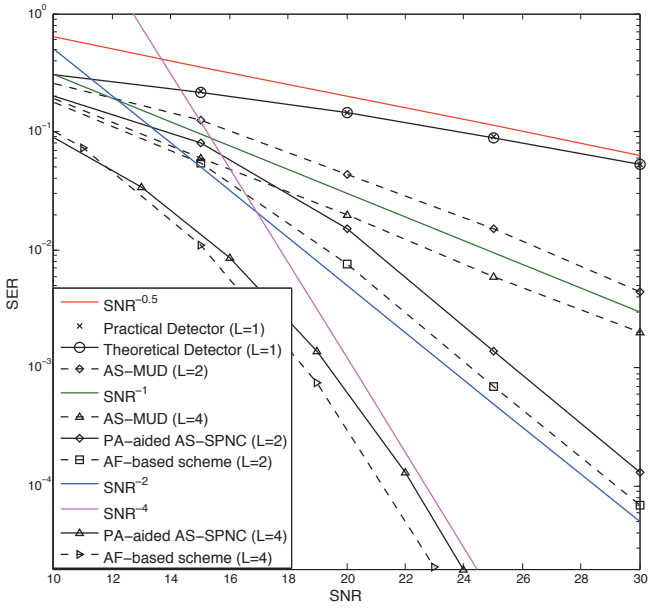

Fig. 2. End-to-End SER performance of AS-SPNC scheme with different number of relay antennas.

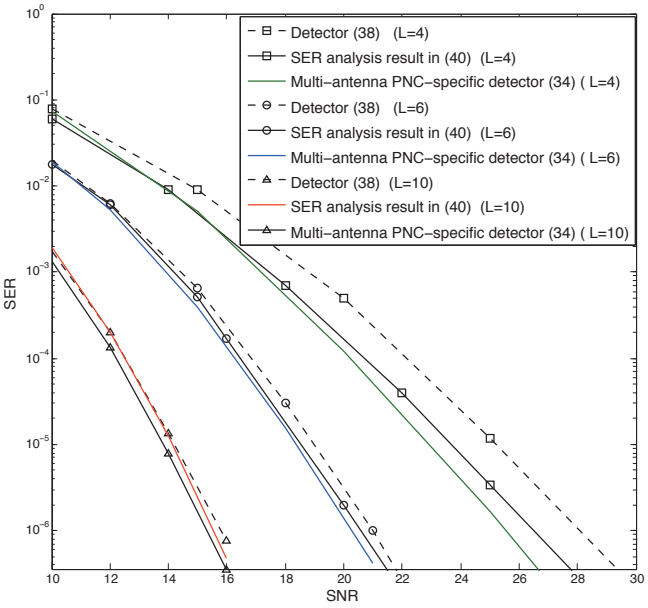

Fig. 3. The SER performance of the SC-SPNC scheme in the MA phase with different number of relay antennas, $M = 8$.

if the SER curve of one scheme tends to be parallel with $\beta SNR^{-\alpha}$, we conclude that a diversity order of α is achieved. Since β does not impact the diversity order, it is neglected in the legend of Fig. 2. Firstly, the performance of the practical PNC-specific detector (16) and that of the theoretical PNC-specific detector (11) in single-antenna TWRC are given. It is observed that the detector (16) achieves nearly the same performance as the theoretical detector (11) while neglecting nn^*, which indicates this approximation is reasonable. Both detectors achieve the diversity order of $\frac{1}{2}$. Then, aided by the PA strategy, the proposed AS-SPNC scheme achieves full diversity in multi-antenna TWRC. However, if PA is not used, applying the maximin-based AS-MUD [29] straightforwardly cannot achieve the full diversity gain. Besides, the AS-SPNC scheme reduces the search space as compared to AS-MUD. For $M = 4$, AS-SPNC has to evaluate 4 possible candidates of s_{NC}, while AS-MUD has to search over 16 possible candidates. Additionally, we give SER curves of the AF-based scheme [13]. The AF-based scheme amplifies the received signal in relay, and achieves better performance than the proposed AS-SPNC. However, the AF-based scheme imposes higher complexity on channel estimation. Specifically, in AF-based scheme the global CSI is assumed to be known to each node. By comparison, in AS-SPNC the source nodes only need to know the local CSI.

Fig. 3 shows the SER of the proposed SC-SPNC in the MA phase, and we set $M = 8$. According to the asymptotic analysis in Section IV-B, the SER performance of (38) and that of (34) will converge to the asymptotic analysis result (40) as L increases. As shown in Fig. 3, when $L = 6$ and $L = 10$, the asymptotic analysis result (40) is tight for the SER of (34) and that of (38). The simulation results also show that SC-SPNC can achieve full diversity.

In Fig. 4 and Fig. 5, we compare the analytical and simulated end-to-end SER performance of SC-SPNC, MUD-PNC and the AF-based schemes. $L = 4$ and $L = 6$ are considered, respectively. It is observed that the analytical SER derived by (46) converges to the simulated result. This observation corroborates the derived analytical expression of (46). The analytical SER expressions for MUD PNC and the AF-based schemes have been given in [12], [32], which validate our simulations for MUD-PNC and for the AF-based schemes. As shown by the simulated curves, the proposed SC-SPNC achieves nearly the same performance as MUD-PNC. However, SC-SPNC reduces the search space. To elaborate a little further, for $M = 8$, SC-SPNC has to evaluate 8 possible candidates of s_{NC}, while MUD-PNC has to search over 64 possible candidates. In addition, SC-SPNC outperforms the AF-based scheme [9]. These observations can be explained by the conclusion provided in Section IV that SC-SPNC, like MRC, combines the information of NCS from all antennas in the effective SIMO system. Similar to the MRC schemes in general SIMO system, SC-SPNC thus achieves both diversity gain and power gain in the MA phase. However, in the AF-based scheme the relay node amplifies its received signal, including the noise, and forwards it to the sources. Consequently, the forwarded noise causes the power loss at the sources. Therefore, SC-SPNC has a power-gain advantage over the AF-based scheme.

VI. Conclusions

This paper investigates SPNC technique which achieves full diversity as MUD-PNC does in multi-antenna TWR networks. However, the search space of MUD-PNC is composed of all the combinations of two modulation constellations. By comparison, the proposed PNC-specific detector reduces the effective search space to a single modulation constellation. The complexity is thus significantly reduced in the proposed schemes. The diversity analysis and asymptotic analysis of SER are given in this paper. The proposed technique can be

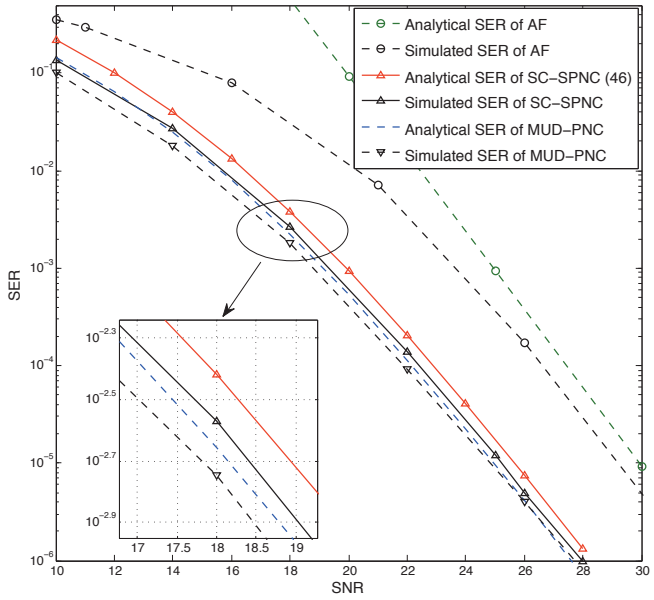

Fig. 4. End-to-End SER performance of AF, MUD-PNC and SC-SPNC schemes with 8PSK, $L = 4$.

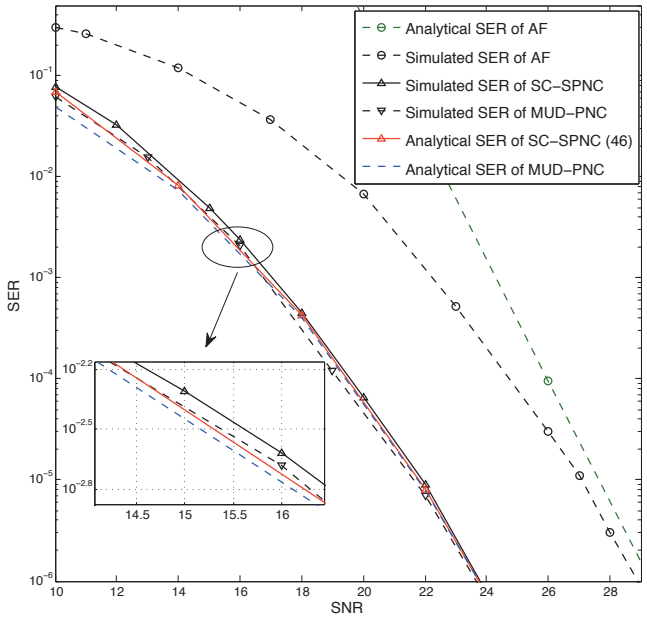

Fig. 5. End-to-End SER performance of AF, MUD-PNC and SC-SPNC schemes with 8PSK, $L = 6$.

applied to some practical systems, like long-term evolution (LTE) system etc. On the other hand, although in this paper the SPNC technique is tailored for MPSK modulation, it is feasible to extend the SPNC to MQAM scenario with a little modification because the MQAM symbol can be expressed as the superposition of constant-amplitude modulated signals. This extension will be addressed in our future work.

APPENDIX A
THE PROOF OF (17)

Proof: The PEP of confusing ϕ_k with $\phi_{k'}$ conditioned on h_1 and h_2 when ϕ_k is intended symbol is written as

$$\Pr\left(\phi_k \to \phi_{k'}|h_1, h_2\right) = \Pr\left\{\Pr\left(yy^* \mid s_{NC} = \phi_k\right)\right\}. \quad (53)$$

Taking the logarithm of $\Pr\left(yy^* \mid s_{NC} = \phi_k\right)$ and $\Pr\left(yy^* \mid s_{NC} = \phi_{k'}\right)$, and considering (15), (53) becomes (47). It should be noted that in (47) $\frac{1}{\sqrt{P}}|h_{\phi_{k'}}|^2\sigma^2\left(\ln\frac{|h_{\phi_{k'}}|^2}{|h_{\phi_k}|^2} - \frac{|2\Re\left(h^*_{\phi_k}\breve{n}\right)|^2}{4|h_{\phi_k}|^2\sigma^2}\right)$ and $\frac{1}{\sqrt{P}}|\Re\left(h^*_{\phi_k}\breve{n}\right)|^2$ are tiny when P is much larger than σ^2. When $SNR \triangleq \frac{P}{\sigma^2}$ is much high, (47) is simplified as

$$\Pr\left(\phi_k \to \phi_{k'}|h_1, h_2\right) = \Pr\left\{\sqrt{P}|\Re\left(\rho\left(\phi_k - \phi_{k'}\right)\right)|^2 + 2\Re\left(\rho\left(\phi_k - \phi_{k'}\right)\right)\Re\left(h^*_{\phi_k}\breve{n}\right) \le 0\right\} \quad (54)$$

Finally, the PEP is given by $\Pr\left(\phi_k \to \phi_{k'}|h_1, h_2\right) = Q\left(\sqrt{\frac{SNR|\Re\left(\rho\left(\phi_k - \phi_{k'}\right)\right)|^2}{2|h_{\phi_k}|^2}}\right)$, where $Q(\cdot)$ is the tail of a Gaussian variable, $Q(x) \triangleq \frac{1}{2\pi}\int_x^\infty \exp\left(-\frac{z^2}{2}\right)dz$. Since $Q(x) \le \exp\left(-\frac{x^2}{2}\right)$ and $|h_{\phi_k}|^2 \le \left(|h_1| + |h_2|\right)^2$, we have

$$\Pr\left(\phi_k \to \phi_{k'}|h_1, h_2\right) \le \exp\left(-\frac{SNR|\Re\left(h_2^* h_1\left(\phi_k - \phi_{k'}\right)\right)|^2}{4\left(|h_1| + |h_2|\right)^2}\right). \quad (55)$$

■

APPENDIX B
THE PROOF OF LEMMA 2

Proof: By averaging with respect to $\xi_{\hat{l}}$, (26) becomes

$$\Pr\left(\phi_k \to \phi_{k'}\right) \le \mathbb{E}_{\xi_{\hat{l}}}\left\{\exp\left(-\frac{SNR\xi_{\hat{l}}|d_{kk'}|^2\cos^2\theta'_{kk'}}{16}\right)\right\}. \quad (56)$$

Since $\xi_l = \min\left\{|h_{1l}|^2, |h_{2l}|^2\right\}$, $|h_{il}|^2$ follows the exponential distribution, hence the probability density function (PDF) of ξ_l can be expressed as $f\left(\xi_l\right) = 2\exp\left(-2\xi_l\right)$. Then, the PDF of $\xi_{\hat{l}}$ may be given by (48). Substituting (48) into (56), we have (49) where $\gamma_{kk'} = \frac{SNR||d_{kk'}||^2\cos^2\theta'_{kk'}}{32}$, and γ_{min} is the minimum of all possible $\gamma_{kk'}$ $(k, k' = 1, \ldots, M)$. Then, the average SER, P_{MA}, is given as $P_{MA} \le (M-1)\frac{L!}{\prod_{l=0}^{l=L-1}\left(\gamma_{\min}SNR+l+1\right)}$. When the SNR is sufficiently high, the diversity order is given by $d_{MA} \geqslant \lim_{SNR\to\infty} -\frac{\log L!(M-1)}{\log SNR} + \lim_{SNR\to\infty}\frac{\sum_{l=0}^{L-1}\log(\gamma_{min}SNR+l+1)}{\log SNR} = L$, which indicates that the diversity order of the proposed scheme is at least L. Note that in MA phase the receiver can at most achieve a diversity order of no more than L [26]. P_{MA} can thus exhibit L diversity orders. ■

APPENDIX C
THE PROOF OF (40)

Proof: When L is sufficiently large, we have $r_{12} = 0$, $r_{11} = ||\mathbf{h}_1||$, and $r_{22} = ||\mathbf{h}_2||$, then r_{11}^2 and r_{22}^2 follow chi-square distribution with the PDF of $f(x) = \frac{1}{(L-1)!}x^{L-1}\exp(-x)$. As a result, the cumulative distribution function (CDF) of z is $F(z) = 1 - \left(\int_z^\infty \frac{1}{(L-1)!}x^{L-1}\exp(-x)\,dx\right)^2$. The probability density of z can be given as (50). Let Γ denote $\frac{SNR|d_{kk'}|^2}{8}$, by substituting (50) into (39), $\Pr\left(\phi_k \to \phi_{k'}\right)$ is written as (51), where $\varpi = \sqrt{\frac{\Gamma}{2+\Gamma}}$. Note that (51) is obtained using the formula for

$$\Pr\left(\phi_k \to \phi_{k'}|h_1,h_2\right)=\Pr\left\{\begin{array}{c}-\frac{1}{\sqrt{P}}|h_{\phi_{k'}}|^2\sigma^2\left(\ln\frac{|h_{\phi_{k'}}|^2}{|h_{\phi_k}|^2}-\frac{|2\Re\left(h_{\phi_k}^*\check{n}\right)||^2}{4|h_{\phi_k}|^2\sigma^2}\right)\geq\\ \sqrt{P}|\Re\left(\rho\left(\phi_k-\phi_{k'}\right)\right)|^2+\frac{1}{\sqrt{P}}|\Re\left(h_{\phi_k}^*\check{n}\right)|^2+2\Re\left(\rho\left(\phi_k-\phi_{k'}\right)\right)\Re\left(h_{\phi_k}^*\check{n}\right)\end{array}\right\}. \tag{47}$$

$$f\left(\xi_{\hat{l}}\right)=2L\exp\left(-2\xi_{\hat{l}}\right)\left(1-\exp\left(-2\xi_{\hat{l}}\right)\right)^{L-1}=2L\sum_{l=0}^{l=L-1}\left(\begin{array}{c}L-1\\ l\end{array}\right)\left(-1\right)^l\exp\left(-2\left(l+1\right)\xi_{\hat{l}}\right). \tag{48}$$

$$\Pr\left(\phi_k\to\phi_{k'}\right)\leq\sum_{l=0}^{l=L-1}\left(\begin{array}{c}L-1\\ l\end{array}\right)\frac{(-1)^lL}{\gamma_{kk'}SNR+l+1}=\frac{L!}{\prod_{l=0}^{l=L-1}\left(\gamma_{kk'}SNR+l+1\right)}<\frac{L!}{\prod_{l=0}^{l=L-1}\left(\gamma_{\min}SNR+l+1\right)}, \tag{49}$$

$$f\left(z\right)=2\left(\sum_{p=0}^{L-1}z^k\frac{\exp\left(-z\right)}{k!}\right)\frac{1}{(L-1)!}z^{L-1}\exp\left(-z\right)=\frac{2}{(L-1)!}\sum_{p=0}^{L-1}z^{L-1+p}\frac{\exp\left(-2z\right)}{p!}. \tag{50}$$

$$\begin{aligned}\Pr\left(\phi_k\to\phi_{k'}\right)&=\mathbb{E}\left(Q\left(\sqrt{2z\Gamma}\right)\right)=\int_0^\infty\int_{\sqrt{2z\Gamma}}^\infty\frac{1}{\sqrt{2\pi}}\exp\left(-\frac{t^2}{2}\right)\frac{2}{(L-1)!}\sum_{p=0}^{L-1}z^{L-1+p}\frac{\exp\left(-2z\right)}{p!}dtdz\\&=\sum_{p=0}^{L-1}\frac{(L-1+p)!}{(L-1)!p!2^{L-1+p}}\int_0^\infty\frac{1}{\sqrt{2\pi}}\exp\left(-\frac{t^2}{2}\right)\left(1-\sum_{q=0}^{L-1+p}\left(\frac{t^2}{\Gamma}\right)^q\frac{\exp\left(-\frac{t^2}{\Gamma}\right)}{q!}\right)dt\\&=\sum_{p=0}^{L-1}\frac{(L-1+p)!}{(L-1)!p!2^{L-1+p}}\left(\frac{1}{2}\left(1-\sum_{q=0}^{L-1+p}\left(\begin{array}{c}2q\\ q\end{array}\right)\varpi\left(\frac{1-\varpi}{2}\right)^q\left(\frac{1+\varpi}{2}\right)^q\right)\right),\end{aligned} \tag{51}$$

$$P_{MA}=\frac{1}{2M}\sum_{k=1}^{M}\sum_{k'=1,\neq k}^{M}\sum_{p=0}^{L-1}\frac{(L-1+p)!}{(L-1)!p!2^{L-1+p}}\left(1-\sum_{q=0}^{L-1+p}\left(\begin{array}{c}2q\\ q\end{array}\right)\varpi\left(\frac{1-\varpi}{2}\right)^q\left(\frac{1+\varpi}{2}\right)^q\right). \tag{52}$$

the even moments of the standard Gaussian distribution with proper scaling. Therefore, the SER is given by (52). ■

APPENDIX D
THE PROOF OF LEMMA 3

Proof: In MUD detector (2), $\sqrt{P}\mathcal{M}\left(w_1\right)\mathbf{h}_1+\sqrt{P}\mathcal{M}\left(w_2\right)\mathbf{h}_2$ can be calculated off-line. The off-line complexity C_{on} for MUD is $14M^2L$. Then, $|\mathbf{y}-\sqrt{P}u_1\mathcal{M}\left(w_1\right)\mathbf{h}_1-\sqrt{P}u_2\mathcal{M}\left(w_2\right)\mathbf{h}_2|^2$ is calculated on-line whose complexity is $5M^2L$. Therefore, the total averaged complexity cost in each symbol duration is given as $C_{mud}=\frac{14M^2L}{N}+5M^2L$. The PNC -Specific detector (34) can be rewritten as

$$\hat{s}_{NC}=\arg\min_{\phi_k\in\Omega}\left(P\sigma^2\ln\det\left(\mathbf{m}\mathbf{m}^H\right)+\left(\mathbf{t}-\mathbf{s}_e\left(\phi_k\right)\right)^T\left(\mathbf{m}\mathbf{m}^H\right)^{-1}\left(\mathbf{t}-\mathbf{s}_e\left(\phi_k\right)\right)\right). \tag{57}$$

Since $\mathbf{m}$ is concerned with $\mathbf{r}_1$,$\mathbf{r}_2$ and s_{NC}, $P\sigma^2\ln\det\left(\mathbf{m}\mathbf{m}^H\right)$ and $\left(\mathbf{m}\mathbf{m}^H\right)^{-1}$ can be calculated at the beginning of each coherence period. It is noted that $\mathbf{m}$ can be written as

$$\mathbf{m}=\left[\begin{array}{cccc}2a&2b&0&0\\ c&0&a&b\\ 0&c&b&-a\end{array}\right],$$

where $a=\Re\left(\mathbf{r}\left(1\right)\right)$, $b=\Im\left(\mathbf{r}\left(1\right)\right)$, and $c=\mathbf{r}\left(2\right)$. Based on the expression of $\mathbf{m}$, we can calculation $P\sigma^2\ln\det\left(\mathbf{m}\mathbf{m}^H\right)$ and $\left(\mathbf{m}\mathbf{m}^H\right)^{-1}$ straightforwardly as

$$P\sigma^2\ln\det\left(\mathbf{m}\mathbf{m}^H\right)=P\sigma^2\ln\det\left(\mathbf{m}\mathbf{m}^H\right)\ln4\left(a^2+b^2+c^2\right)\cdot\cdot\left(a^2+b^2\right)^2$$

TABLE II
COMPLEXITY COMPARISON BETWEEN MUD AND PNC-SPECIFIC DETECTOR

	OPERATION	COMPLEXITY
off-line	QR decomposition, i.e., $\mathbf{Q}_1$ and $\mathbf{R}$. $\mathbf{Q}=\mathbf{R}^{-1}\tilde{\mathbf{H}}$ and $\mathbf{C}=P\left(\mathbf{r}_1\mathbf{r}_1^H+\mathbf{r}_2\mathbf{r}_2^H\right)$	$31L+9$
	Calculate $\mathbf{s}_e\left(\phi_k\right)$, $P\sigma^2\ln\det\left(\mathbf{m}\mathbf{m}^H\right)$ and $\left(\mathbf{m}\mathbf{m}^H\right)^{-1}$	$47M$
on-line	Signal Combination, calculate $\widetilde{\mathbf{y}}\widetilde{\mathbf{y}}^H$, and remove $\mathbf{C}$	$16L+8$
	$P\sigma^2\ln\det\left(\mathbf{m}\mathbf{m}^H\right)+\left(\mathbf{t}-\mathbf{s}_e\left(\phi_k\right)\right)^T\left(\mathbf{m}\mathbf{m}^H\right)^{-1}\left(\mathbf{t}-\mathbf{s}_e\left(\phi_k\right)\right)$	$21M$

and $\left(\mathbf{m}\mathbf{m}^H\right)^{-1}$ is given as

$$\left[\begin{array}{ccc}\frac{a^2+b^2+c^2}{4\left(a^2+b^2\right)^2}&-\frac{ac}{2\left(a^2+b^2\right)^2}&-\frac{bc}{2\left(a^2+b^2\right)^2}\\ -\frac{ac}{2\left(a^2+b^2\right)^2}&\frac{\left(a^2+b^2\right)^2+a^2c^2}{\left(a^2+b^2+c^2\right)\left(a^2+b^2\right)^2}&\frac{abc^2}{\left(a^2+b^2+c^2\right)\left(a^2+b^2\right)^2}\\ -\frac{bc}{2\left(a^2+b^2\right)^2}&\frac{abc^2}{\left(a^2+b^2+c^2\right)\left(a^2+b^2\right)^2}&\frac{\left(a^2+b^2\right)^2+b^2c^2}{\left(a^2+b^2+c^2\right)\left(a^2+b^2\right)^2}\end{array}\right].$$

On the other hand, since only $\mathbf{T}_0\left(1,1\right)$ and $\mathbf{T}_0\left(1,2\right)$ are used by the PNC-specific detector, $\mathbf{T}_0\left(2,2\right)$ does not contain any information of s_{NC}, only $\widetilde{\mathbf{y}}\left(1\right)\widetilde{\mathbf{y}}\left(1\right)^*=||\widetilde{\mathbf{y}}\left(1\right)||^2$ and $\widetilde{\mathbf{y}}\left(1\right)\widetilde{\mathbf{y}}\left(2\right)^*$ are needed. Correspondingly, in $\mathbf{C}=P\left(\mathbf{r}_1\mathbf{r}_1^H+\mathbf{r}_2\mathbf{r}_2^H\right)$, only $\mathbf{C}\left(1,1\right)$ and $\mathbf{C}\left(1,2\right)$ are needed, Then, we give the detailed FLOPs step by step in the TABLE II. According to TABLE II, $C_{pnc}=\frac{47M+31L+9}{N}+21M+16L+8$.

■

REFERENCES

[1] P. Larsson, N. Johansson, and K. Sunell, "Coded bidirectional relaying," in *Proc. 2006 IEEE Vehicular Technology Conference – Spring*, pp. 851–855.

[2] S. Kim, N. Devroye, P. Mitran, and V. Tarokh, "Achievable rate regions and performance comparison of half duplex bi-directional relaying protocols," *IEEE Trans. Inf. Theory*, vol. 57, no. 10, pp. 6405–6418, 2011.

[3] S. Kim, P. Mitran, and V. Tarokh, "Performance bounds for bi-directional coded cooperation protocols," *IEEE Trans. Inf. Theory*, vol. 54, no. 11, pp. 5235–5241, 2008.

[4] B. Rankov and A. Wittneben, "Spectral efficient signaling for half-duplex relay channels," in *Proc. 2005 Asilomar Conference on Signals, Systems and Computer*, pp. 1066–1071.

[5] E. V. der Meulen, "Three terminal communication channels," *Advances in Applied Probability*, vol. 3, pp. 120–154, 1971.

[6] S. Li, R. Yeung, and N. Cai, "Linear network coding," *IEEE Trans. Inf. Theory*, vol. 49, no. 2, pp. 371–381, 2003.

[7] D. Gunduz, A. Goldsmith, and H. Poor, "MIMO two-way relay channel: diversity-multiplexing tradeoff analysis," in *Proc. 2008 Asilomar Conference on Signals, Systems and Computer*, pp. 1474–1478.

[8] C. Yuen, W. H. Chin, Y. L. Guan, W. Chen, and T. Tee, "Bi-directional multi-antenna relay communications with wireless network coding," in *Proc. 2008 IEEE Vehicular Technology Conference – Spring*, pp. 1385–1388.

[9] Y. Jing, "A relay selection scheme for two-way amplify-and-forward relay networks," in *Proc. 2009 International Conference on Wireless Communications and Signal Processing*, pp. 1–5.

[10] L. Song, G. Hong, B. Jiao, and M. Debbah, "Joint relay selection and analog network coding using differential modulation in two-way relay channels," *IEEE Trans. Veh. Technol.*, vol. 59, no. 6, pp. 2932–2939, 2010.

[11] M. Eslamifar, C. Yuen, W. Chin, and Y. Guan, "Max-Min antenna selection for bi-directional multi-antenna relaying," in *Proc. 2010 IEEE Vehicular Technology Conference – Spring*, pp. 1–5.

[12] M. Eslamifar, W. Chin, W. Hau, C. Yuen, and Y. Guan, "Performance analysis of two-step bi-directional relaying with multiple antennas," *IEEE Trans. Wireless Commun.*, vol. 11, no. 12, pp. 4237–4242, Dec. 2012.

[13] Z. Ding, K. Leung, D. Goeckel, and D. Towsley, "On the study of network coding with diversity," *IEEE Trans. Wireless Commun.*, vol. 8, no. 3, pp. 1247–1259, 2009.

[14] H. Gao, T. Lv, S. Zhang, C. Yuen, and S. Yang, "Zero-forcing based MIMO two-way relay with relay antenna selection: transmission scheme and diversity analysis," *IEEE Trans. Wireless Commun.*, vol. 11, no. 12, pp. 4426–4437, 2012.

[15] S. Zhang, S. Liew, and P. Lam, "Hot topic: physical-layer network coding," in *Proc. 2006 International Conference on Mobile Computing and Networking*, pp. 358–365.

[16] L. Lu, S. C. Liew, and S. Zhang, "Physical-layer network coding: tutorial, survey, and beyond," *Physical Commun.*, 2012.

[17] T. Koike-Akino, P. Popovski, and V. Tarokh, "Optimized constellations for two-way wireless relaying with physical network coding," *IEEE J. Sel. Areas Commun.*, vol. 27, no. 5, pp. 773–787, 2009.

[18] H. Yang, Y. Choi, and J. Chun, "Modified high-order PAMs for binary coded physical-layer network coding," *IEEE Commun. Lett.*, vol. 14, no. 8, pp. 689–691, 2010.

[19] M. Noori and M. Ardakani, "On symbol mapping for binary physical-layer network coding with PSK modulation," *IEEE Trans. Wireless Commun.*, vol. 59, no. 99, pp. 1–6, 2012.

[20] T. Cui and J. Kliewer, "Memoryless relay strategies for two-way relay channels: performance analysis and optimization," in *Proc. 2008 IEEE International Conference on Communications*, pp. 1139–1143.

[21] T. Cui, T. Ho, and J. Kliewer, "Memoryless relay strategies for two-way relay channels," *IEEE Trans. Commun.*, vol. 57, no. 10, pp. 3132–3143, 2009.

[22] H. Gao, X. Su, and T. Lv, "Combined MRC-like reception and transmit diversity for physical-layer network coding with multiple-antenna relay," in *Proc. 2011 International Conference on Telecommunications*, pp. 1–5.

[23] R. Cao, T. Lv, F. Long, and H. Gao, "Symbol-based physical-layer network coding with MPSK modulation," in *Proc. 2011 IEEE GLOBECOM*, pp. 1–5.

[24] R. Cao, T. Lv, and H. Gao, "Symbol-based physical-layer network coding for two-way relay channel," in *Proc. 2011 IEEE MILCOM*, pp. 1–6.

[25] J. Proakis, *Digital Communications*. McGraw-Hill, 2001.

[26] D. Tse and P. Viswanath, *Fundamentals of Wireless Communication*. Cambridge University Press, 2005.

[27] U. Erez and R. Zamir, "Achieving 1/2 log (1+ SNR) on the AWGN channel with lattice encoding and decoding," *IEEE Trans. Inf. Theory*, vol. 50, no. 10, pp. 2293–2314, 2004.

[28] H. Gao, X. Su, T. Lv, R. Cao, and T. Wang, "Achieving diversity for physical-layer network coding based two-way multiple-antenna relay: a two-phase diversity scheme," *IEICE Trans. Commun.*, vol. E94-B, no. 12, pp. 3382–3386, 2011.

[29] I. Krikidis, "Relay selection for two-way relay channels with MABC DF: a diversity perspective," *IEEE Trans. Veh. Technol.*, vol. 59, no. 9, pp. 4620–4628, 2010.

[30] T. Duong, C. Yuen, H.-J. Zepernick, and X. Lei, "Average sum-rate of distributed Alamouti space-time scheme in two-way amplify-and-forward relay networks," in *Proc. 2010 IEEE GLOBECOM Workshops*, pp. 79–83.

[31] A. Papoulis and R. Probability, *Stochastic Processes, Vol. 3*. McGraw-Hill, 1991.

[32] L. Song, "Relay selection for two-way relaying with amplify-and-forward protocols," *IEEE Trans. Veh. Technol.*, vol. 60, no. 4, pp. 1954–1959, 2011.

Ruohan Cao received her B.Eng. degree in 2009 from Shandong University of Science and Technology (SDUST), Qingdao, China. She is currently working towards her Ph.D degree in Beijing University of Posts and Telecommunications (BUPT), Beijing, China. From November 2012, she also served as a research assistant for the Department of Electrical and Computer Engineering at University of Florida, supported by the China Scholarship Council. Her research interests include physical-layer network coding, multiuser multiple-input-multiple-output systems and physical-layer security.

Tiejun Lv (M'08-SM'12) received the M.S. and Ph.D. degrees in electronic engineering from the University of Electronic Science and Technology of China, Chengdu, China, in 1997 and 2000, respectively. From January 2001 to December 2002, he was a Postdoctoral Fellow with Tsinghua University, Beijing, China. From September 2008 to March 2009, he was a Visiting Professor with the Department of Electrical Engineering, Stanford University, Stanford, CA. He is currently a Professor with the School of Information and Communication Engineering, Beijing University of Posts and Telecommunications. He is the author of more than 100 published technical papers on the physical layer of wireless mobile communications. His current research interests include signal processing, communications theory and networking. Dr. Lv is also a Senior Member of the Chinese Electronics Association. He was the recipient of the "Program for New Century Excellent Talents in University" Award from the Ministry of Education, China, in 2006.

Hui Gao (S'10-M'13) received his B.S. degree in Information Engineering and Ph.D. degree in Signal and Information Processing from Beijing University of Posts and Telecommunications (BUPT), Beijing, China, in July 2007 and July 2012, respectively. From May 2009 to June 2012, he also served as a research assistant for the Wireless and Mobile Communications Technology R&D Center, Tsinghua University, Beijing, China. From April 2012 to June 2012, he visited Singapore University of Technology and Design (SUTD), Singapore, as a research assistant. Since July 2012, he has been with SUTD as a Postdoc Researcher. His research interests include ultra-wideband wireless communications, physical-layer network coding and multiuser multiple-input-multiple-output systems.

Shaoshi Yang (S'09-M'13) received the B.Eng. Degree in information engineering from Beijing University of Posts and Telecommunications, Beijing, China, in 2006. He is currently working toward the Ph.D. degree in wireless communications with the School of Electronics and Computer Science, University of Southampton, Southampton, U.K., through scholarships from both the University of Southampton and the China Scholarship Council. From November 2008 to February 2009, he was an Intern Research Fellow with the Communications Technology Laboratory, Intel Labs China, Beijing, where he focused on Channel Quality Indicator Channel design for mobile WiMAX (802.16 m). His research interests include multiuser detection/multiple-input–mutliple-output (MIMO) detection, multicell joint/distributed processing, cooperative communications, green radio, and interference management. He has published in excess of 20 research papers on IEEE journals and conferences. Shaoshi is a recipient of the PMC-Sierra Telecommunications Technology Scholarship, and a Junior Member of the Isaac Newton Institute for Mathematical Sciences, Cambridge, UK. He is also a TPC member of both the 23rd Annual IEEE International Symposium on Personal, Indoor and Mobile Radio Communications (IEEE PIMRC 2012), and of the 48th Annual IEEE International Conference on Communications (IEEE ICC 2013).

John M. Cioffi - BSEE, 1978, Illinois; PhDEE, 1984, Stanford; Bell Laboratories, 1978-1984; IBM Research, 1984-1986; EE Prof., Stanford, 1986-present, now emeritus. Cioffi founded Amati Com. Corp in 1991 (purchased by TI in 1997) and was officer/director from 1991-1997. He currently also is on the Board of Directors of ASSIA (Chairman and CEO), Alto Beam, and the Marconi Foundation. Cioffi's specific interests are in the area of high-performance digital transmission. Cioffi is the recipient of the IEEE's Alexander Graham Bell and Millenium Medals (2010 and 2000); Economist Magazine 2010 Innovations Award; International Marconi Fellow (2006); Member, US National and UK Royal Academies of Engineering (2001, 2009); IEEE Kobayashi Medal (2001); IEEE Fellow (1996); IEE JJ Tomson Medal (2000); 1999 and 2010 U. of Illinois Outstanding Alumnus, 1991 and 2007 IEEE Comm. Mag. best paper; 1995 ANSI T1 Outstanding Achievement Award; NSF Presidential Investigator (1987-1992); and numerous Conference Best-Paper awards. Cioffi has published over 400 papers and holds over 100 patents, of which many are heavily licensed including key necessary patents for the international standards in ADSL, VDSL, DSM, and WiMAX.